Experimental Study on Masonry Infill Walls under Blast Loading

PEREIRA, JOÃO[1]; CAMPOS, JOSÉ[2]; LOURENÇO, PAULO B.[3]

ABSTRACT: The vulnerability of the masonry envelop under blast loading is considered critical due to the risk of loss of lives. The dynamic behaviour of masonry infill walls subjected to dynamic out-of-plane loading was experimentally investigated in this work. Confined underwater blast wave generators (WBWG) allows applying an extremely high rate conversion of the explosive detonation energy into the kinetic energy of a thick water confinement, which, in turn, allows a surface area distribution avoiding the generation of high velocity fragments and reducing atmospheric sound wave. In the present study water plastic containers, having in its centre a detonator inside a cylindrical explosive charge, were used. Tests were performed in unreinforced walls with 1.7 by 3.5 m, which are 1:1.5 scaled. Besides the usage of pressure and displacement transducers, pictures were recorded with high-speed video cameras to process the deflections and identify failure modes.

Keywords: Infill walls, Out-of-plane loading, Blast loading, WBWG

1   INTRODUCTION

Very few numerical or experimental studies have been conducted on impact and blast on structural components of building structures, characterized by strain rates well over 1 s^{-1}, with quasi-static tests characterized by strain rates in the range 10^{-5} to 10^{-7} s^{-1}. This calls for more research to obtain an accurate representation of the effect of blasts, as high nonlinear behaviour and possible brittle failure has been observed. The vulnerability of structures under dynamic actions has been emphasized by many studies, most of them performed to mitigate seismic risk. The out of plane vulnerability of the masonry envelop under dynamic loading is considered critical due to the risk of loss of lives, emphasized by many studies, particularly in the case of earthquakes [1] and explosion debris [2]. Still, only a few laboratory experimental investigations are available, simulating vehicles impacts on parapets [3] and air-blasting [4].

The main issue on the mechanical behaviour under blast is the strength increase due to high-strain rate. Explosions produce very high strain rates, usually around $10^2 - 10^4$ s^{-1}. Reinforced concrete structures, for example, are highly affected by this phenomenon. Its resistance can increase greatly due to the high strain rate effect, dynamic increase factor as high as 4 in compression and 6 in tension have been reported [5][6]. In the case of masonry and its components the available studies are very limited. Recently, dynamic increase factors higher than 2 in compression for clay brick were reported [7][8].

[1] PhD Student, ISISE, Department of Civil Engineering, jpereira@civil.uminho.pt
[2] Professor, University of Coimbra, Department of Mechanical Engineering, andrade.campos@dem.uc.pt
[3] Full Professor, ISISE, Department of Civil Engineering, pbl@civil.uminho.pt

This work intends to present a newly developed test setup for testing out-of-plane walls under dynamic loading using underwater blast wave generators. Underwater blasting operations have been, during the last decades, subject of research and development of maritime blasting operations (including torpedo studies), of aquarium tests for the measurement of blasting energy of industrial explosives and of confined underwater blast wave generators (WBWG). WBWGs allow a wide range of produced blast impulses and surface area distributions. This technique avoids also the generation of high velocity fragments and reduces atmospheric sound wave [9][10].

2   TEST SETUP

This work was performed in collaboration with LEDap (Laboratory of Energetics and Detonics) in Condeixa-a-Nova, Portugal. The developed test setup was constructed at LEDap facilities and comprises several elements. A support steel structure holds the structural element in place and provides sufficient reaction to the wall's reinforced concrete frame. On one side of the wall a number of large (one cubic metre) water containers are placed to act as WBWG and apply the desired load. On the other side of the wall, measuring equipment is placed is order to obtain the required behaviour of the wall. The maximum deflection is measured using laser and high speed video equipment, which was used to study the behaviour of the wall during the test, 0a. This area is surrounded by protection walls and a safe area was placed to provide secured hosting for the acquisition equipment and personal during the tests, 0b.
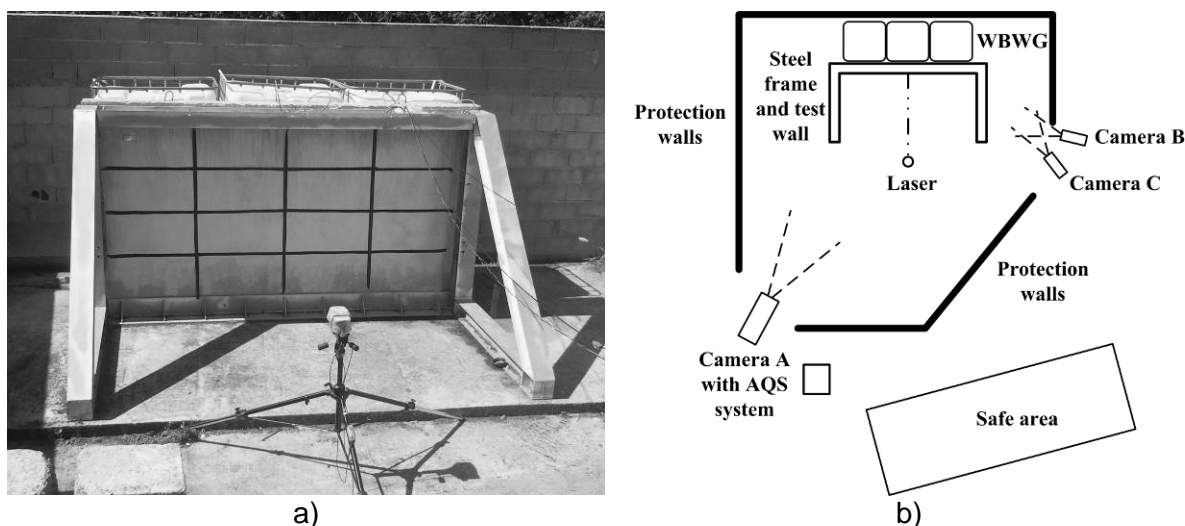

Figure 1.   Final configuration of the test site: a) supporting structure and wall; b) test setup layout.

2.1. Blast wave generator

The original blast wave generators (BWG), from the direct application of an explosion in air of high explosives, have the inconvenient of hot polluted gases products, a reduced area of induced pressure, the possibility of generation of high velocity fragments and the existing of a very intense sound wave [9]. Since physical properties of water and air are different, the characteristics of the shock waves (in air and water) are different, mainly due to the differences of density and shock wave velocity (shock impedance). The density of water is about 800 times greater than the density of air; the sound velocity in water is 1500 m/s and in air ~330 m/s (4.5 times slower). Shock wave in water is 4.5 times faster than in air; pressure impulse in shock wave in water is 15-20 times higher than in air [10]. After the detonation of an explosive charge under water, the detonation products expand generating a shock wave in water and forming a gas bubble. Gas bubble expands and pressure inside the bubble decreases. Because of inertia of water flow in front of the bubble, the expansion of gas bubble continues even after the slightly decrease of pressure inside the bubble to a value below

pressure of the surrounding water. Afterwards, the pressure inside the gas bubble drops below pressure of surrounding water and gas bubble movement stops. However the phenomenon does not stops - gas bubble contracts under the action of surrounding pressure. The contractions and expansions continues (several cycles) generating, by this way, pulsating movement of gas bubble and additional compression waves in the water [9][10]. This kind of evolutions is very important in large volumes, but in our case it must be reduced or even eliminated – in this case the water should be used just as a pressure dissipative medium, see Figure 2.
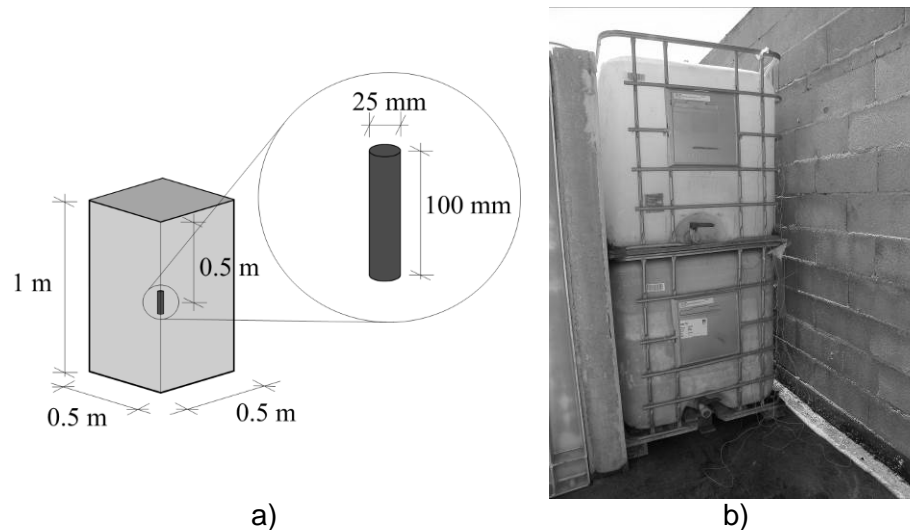

a)   b)

Figure 2. WBWG: a) explosive charge location; b) placing the water container in the final position.

2.2. Pressure/deflection acquisition

One of the main issues regarding dynamic testing, blast loading in this case, is the proper acquisition of signals. The measuring equipment needs to have capacity for high acquisition rates. In this work there were two signals that need to be recorded: a) the pressure profile acting on the wall; and b) the deflection profile of the wall.

For the pressure acquisition, a new sensor was developed for these tests. The mechanism used to measure the pressure consists in an assembled instrumental stainless steel plate between the wall and the water container. The pressure setup is a pressure tube connected to a pressure sensor. This tube contains thin oil and is connected in a closed loop, Figure 3. The pressure device works like a force multiplier justified by the hydrostatic pressure transmission. The pressure sensors used were 4-20 mA Gems[TM] Sensors and Controls 3100B0016G01B and 3100B0010B01B. The connection of the sensor to the periphery equipment can be seen in Figure 4. In order to plot the acquired pressure signal, these sensors were connected to Tektronix TDS 320 oscilloscopes. This sensor was previously tested and calibrated [9][10].
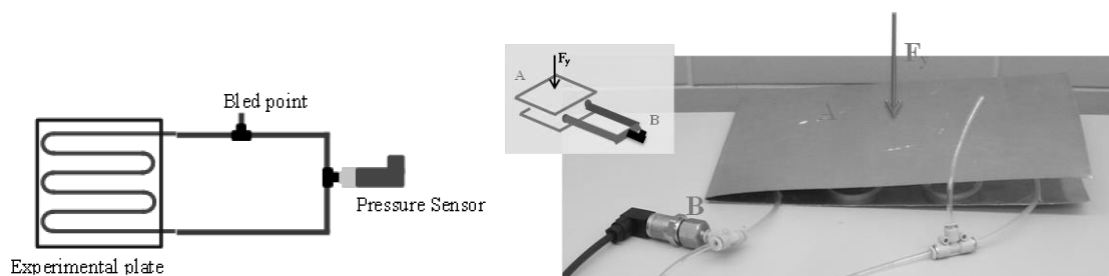

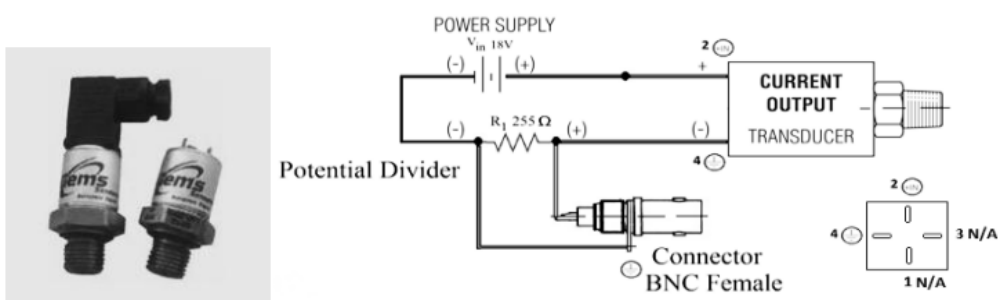**Figure 3.** Pressure sensor schematics and construction.

Figure 4. Pressure sensor connections to the periphery equipment.

For the deflection acquisition, a Keyence CMOS Multi-Function analogue laser sensor IL-2000 with a signal amplifier IL-1000 was used. This sensor was connected to a National Instruments acquisition system composed of a SCXI-1000DC chassis, a SCXI-1600 data acquisition and control card for PC connection and a generic input module SCXI-1520 with a SCXI-1314 mount. In this case the sampling speed was limited by the laser sensor and was set as 3 kHz. With this system, it is only possible to measure the deflection of one point in the wall.
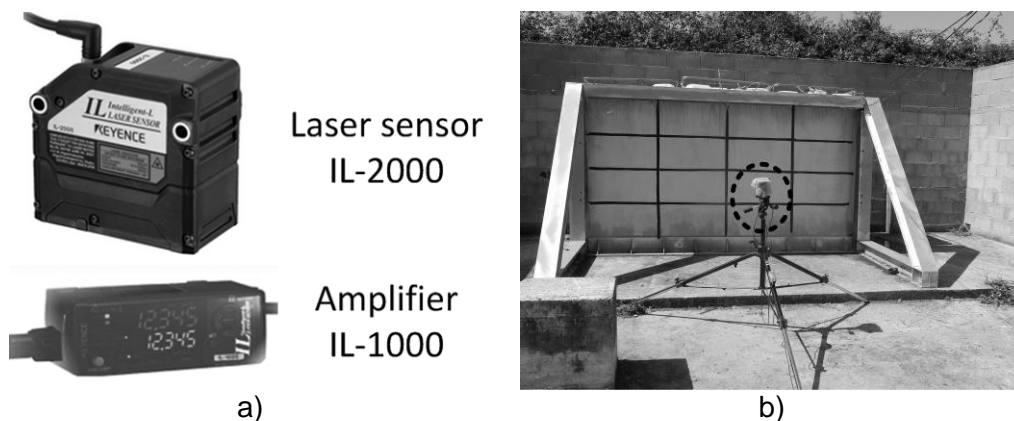

Figure 5. Deflection acquisition: a) laser sensor and amplifier; b) laser mounted in place.

Besides the usage of pressure and displacement transducers, high speed video equipment was used to study the behaviour of the wall during the test. Three different cameras were used, marked in 0b as camera A, B and C. Camera A is a PHOTRON APX-RS and was placed to have a full view of the wall. This camera was set with an acquisition frequency of 1 kHz. Cameras B and C are Casio EX-FH25 and were placed with different views. Camera B was placed on the side of the wall in order to capture the profile of the wall. Camera C was placed in order to capture the WBWG and their behaviour during the test. Both these two cameras were set with an acquisition frequency of 0.4 kHz. To help having a better view of the movement of the wall, a regular mesh was drawn in the wall using black tape, 0b.

3 UNREINFORCED INFILL WALL

The first specimen tested with this new developed test setup was an unreinforced masonry wall. This wall was a 3.5 x 1.7 m^2 masonry panel inside a reinforced concrete frame with a thickness of 180 mm, 150 mm from the hollow clay block and 15 mm on each side from plaster. This wall specimen, Figure 6, was tested previously in different condition and additional details on the composition and the construction procedure of this specimen can be found in [11][12].
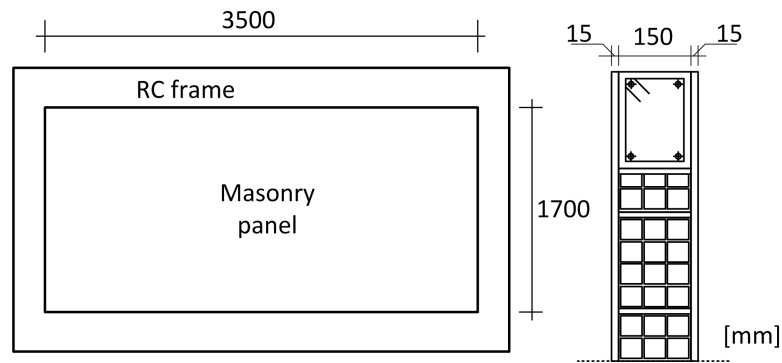
Figure 6. Masonry infill panel schematic and geometry.

After the test, the acquired signals need to be processed. From the oscilloscopes the applied pressure on the wall was obtained and the final pressure profile was plotted, Figure 7. The pressure rises to 149 kPa in the first 6 ms, then decays and reaches 119 kPa at 17.5 ms and stops acting after 29 ms. From the laser sensor, the deflection on the central point of the wall was obtained, Figure 8. The deflection on the wall has an expected profile, increasing until its maximum of 14.6 mm after 24 ms and has a residual deformation of around 10 mm. Besides these profiles, the cracks on the wall panel were marked for comparison with the numerical models, Figure 9. There is a large concentration of large horizontal cracks at the centre of the wall and these spread to the corner as they move away from the centre. There are also some large cracks at the top support edge. These results were used to calibrate numerical models able to simulate these extreme dynamic situations, which allow having a more detailed study on these structural elements.
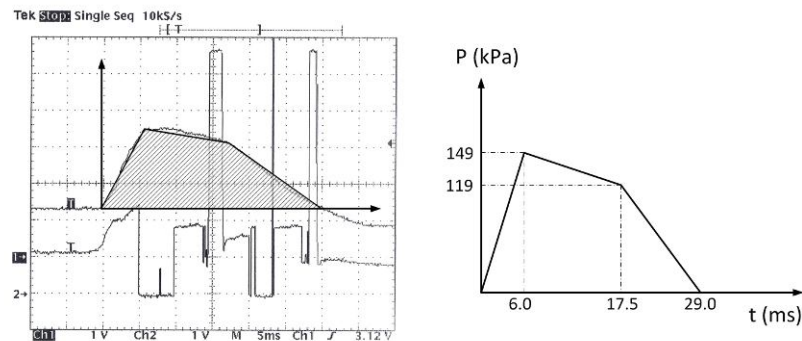

Figure 7. Acquired pressure from the oscilloscope and the final pressure profile.
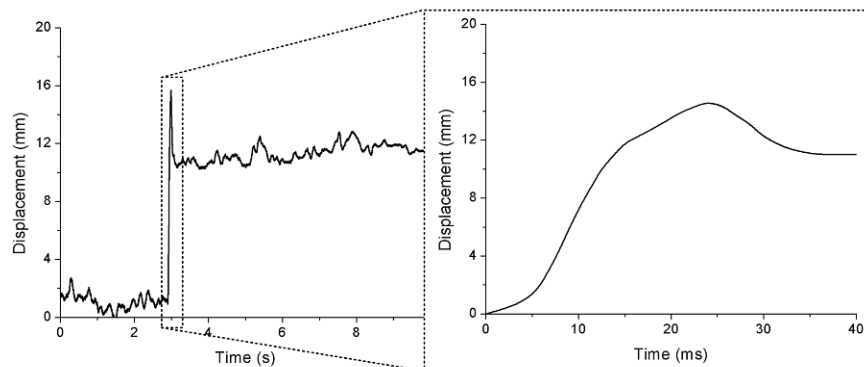

Figure 8. Displacement at midpoint acquired with laser.
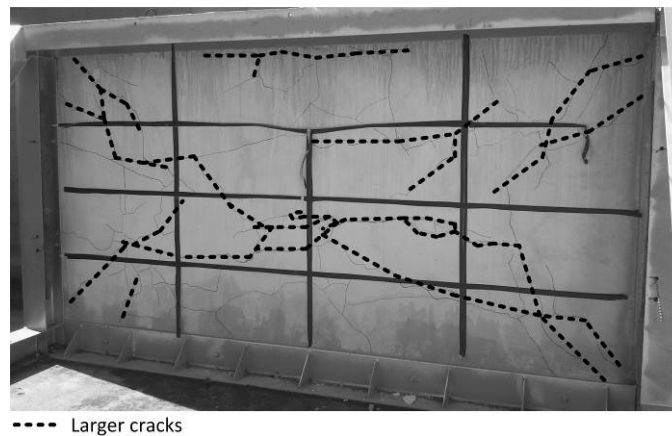
---- Larger cracks

Figure 9. Damaged wall after blast test.

4 NUMERICAL MODELLING

The FEM model was built in the ABAQUS software [13], where the Explicit solver was used. This software has been used successfully in previous situation regarding similar loading conditions [14][15][16] and similar materials [17][18]. This wall was discretized with 8 nodes solid elements (C3D8R) with reduced integration and hourglass control [13]. The final mesh was automatically generated by ABAQUS, and then manipulated and controlled in order to obtain a good quality mesh. Only the infill masonry was modelled and all edges were considered constrained in all degrees of freedom. The thickness of the wall was set as 180 mm (brick plus plaster). The final mesh has 4872 elements and 6844 nodes

The CDP (Concrete Damaged Plasticity) material model used in ABAQUS software is a modification of the Drucker-Prager strength hypothesis. The CDP model requires the definition of five parameters: a) the dilation angle (Ψ); b) the flow potential eccentricity (ε); c) the ratio of initial equibiaxial compressive yield stress to initial uniaxial compressive yield stress (fb0/fc0); d) the viscosity parameter (μ); e) and the parameter K_c. For all these five parameters the default values suggested in [13] were used, being: 40º, 0.1, 1.16, 0.0 and 0.667 respectively. The CDP model assumes that the failure in both tensile cracking and compressive crushing of the material is characterized by damage plasticity. It uses the concept of isotropic damage evolution in combination with isotropic tensile and compressive plasticity to represent the inelastic and fracture behaviour of the material. It allows the definition of strain hardening in compression and strain softening in tension. The adopted stress-strain curves in tension and compression can be seen in Figure 10. Additional information regarding this material model can be found in [19][20][21][22].

Table 1 presents the static mechanical properties for this masonry infill wall and were obtained from [12]. These values served as a base for the calibration of the numerical model. The dynamic properties were obtained by calibrating the numerical model to match the deflection behaviour of the experimental wall. The final dynamic properties and the respective dynamic increase factor (DIF), which is the relation between the dynamic properties and its static reference, can be seen in Table 1.

Figure 11a shows the result of the numerical model and compares it with the experimental results. There is a good initial agreement up until 12 mm in deformation. At this instant the experimental curve changes its slope, probably due to appearing cracks. The maximum displacement has a difference of 3%. In the post-peak behaviour there is a considerable difference between the experimental and the numerical model. In the experimental test the wall was able to set its residual deformation at 76% of the maximum deformation. In the numerical model the residual deformation was 91%. In the experimental test, when the blast wave from the WBWG reaches the wall it generates an expansion

wave that travels through the thickness of the wall. When this expansion wave reaches the opposite edge of the wall it will start moving in the opposite direction creating a "negative" wave profile, which was not considered in the numerical model. When the structural element reaches a high level of deformation this effect can be neglected, due to the lack of capacity of the element to sustain this expansion wave in the opposite direction.
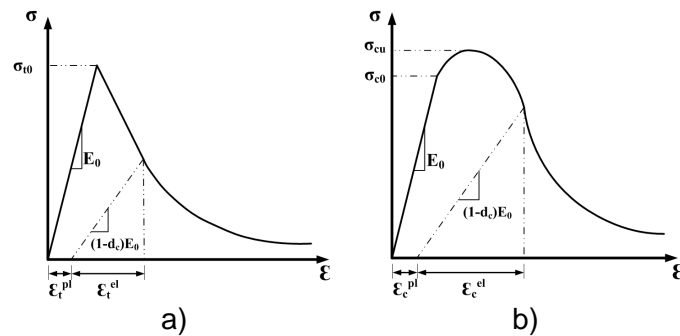

Figure 10. Stress-strain relations: a) in tension; b) in compression [19].

Table 1. Mechanical properties for masonry wall.

Masonry	Ref.	Calibrated	DIF
Compressive Strength (f_c) [MPa]	1.26	3.78	3
Tensile Strength (f_t) [MPa]	0.125	0.375	3
Mode I-fracture energy (G_f^I) [N/mm]	0.012	0.025	2
Young's Modulus (E) [GPa]	3.6	7.2	2

A proper definition of the mechanical properties through the dynamic increase factor is crucial in this type of analysis. As can be seen in Figure 11b, where a comparison of the dynamic increase factor is performed, using the static properties (DIF = 1) in this model results in excessive deformation which would results in the collapse of the wall. On the other hand, using a dynamic increase factor of 5 in all mechanical properties the wall behaves mostly in its elastic regime, having a neglectable residual deformation.
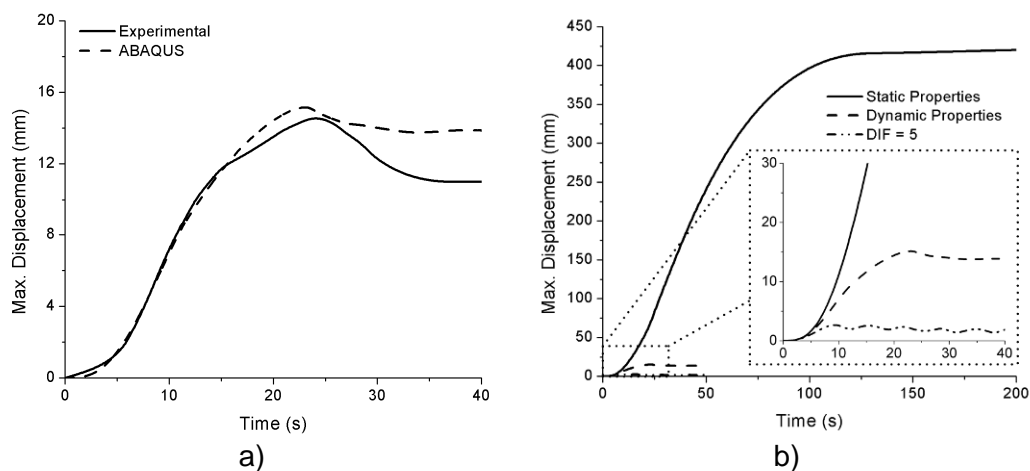

Figure 11. Numerical results: a) Comparison between the numerical and experimental results; b) Influence of the dynamic increase factors on the behaviour of the wall.

Besides the comparison of the deflection profile, the damage on the wall was also compared. In order to have an approximation on where the cracks would appear, the maximum principal plastic

strains were plotted, Figure 12. As expected, according to this model, there is a concentration of cracks at mid height of the wall that will start to spread to the corners as we move further from the centre point. There is also some damage at the bottom and top edge of the wall. These results are in agreement with the observed damage in the experimental test, Figure 9.
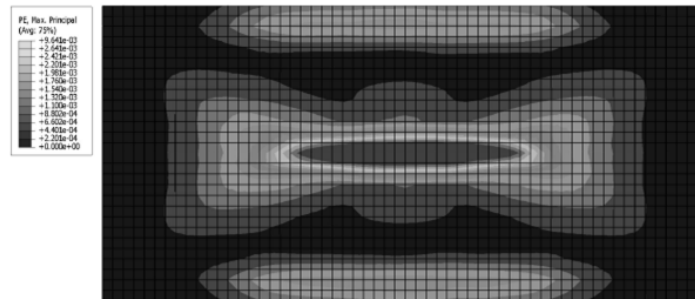

Figure 12. Maximum principal plastic strains.

4.1. Parametric study

A parametric study was performed on the mechanical and geometric properties of unreinforced masonry infill panels. The results are summarized in Figure 13. The maximum displacement is plotted against the scaled distance, Z:

$$Z = \frac{R}{W^{1/3}}$$

(1)

where R = distance to the explosive and W = mass of the explosive in TNT equivalent.

To create the pressure profiles when varying the weight of the explosive or the distance, a set of empirical solution are available in the literature. The pressure profile was assumed to be with a triangular shape with the maximum pressure at the initial time and decaying in pressure until the positive duration (t_d). Equations (2) to (4) show how to determine the incident over-pressure (P_{s0}), the reflected pressure (P_r) and the positive phase duration (t_d). Additional details on these equations can be found in [23][24].

$$P_{S0} = 6784 \frac{W}{R^3} + 93 \left(\frac{W}{R^3} \right)^{\frac{1}{2}}$$

(2)

$$P_r = 2P_{S0} \left(\frac{7P_0 + 4P_{S0}}{7P_0 + P_{S0}} \right)$$

(3)

$$t_D = 10.23 \frac{W^{1/3}}{\sqrt{P_{SO}}}$$

(4)

Here P_0 = ambient pressure.

The compressive strength, Figure 13a, has a considerable influence on the maximum displacement of the wall, for smaller scaled distances. This influence appears to fade once a certain level of compressive strength is achieved. Meaning that from a certain point there is no real advantage on increasing the compressive strength. The same conclusion can be obtained when analysing the tensile strength, Figure 13b. When varying the tensile strength, the fracture energy was also changed in the same proportion as the tensile strength. The Young's modulus, Figure 13c, influences the maximum displacement of the wall at all levels of scaled distance. The Mode I-fracture

energy, Figure 13d, only influences the maximum displacement at smaller scaled distances. Here, the tensile strength was kept the same for all models. The thickness of the wall, Figure 13e, is obviously one of the parameters with larger influence on the maximum displacement of the wall.
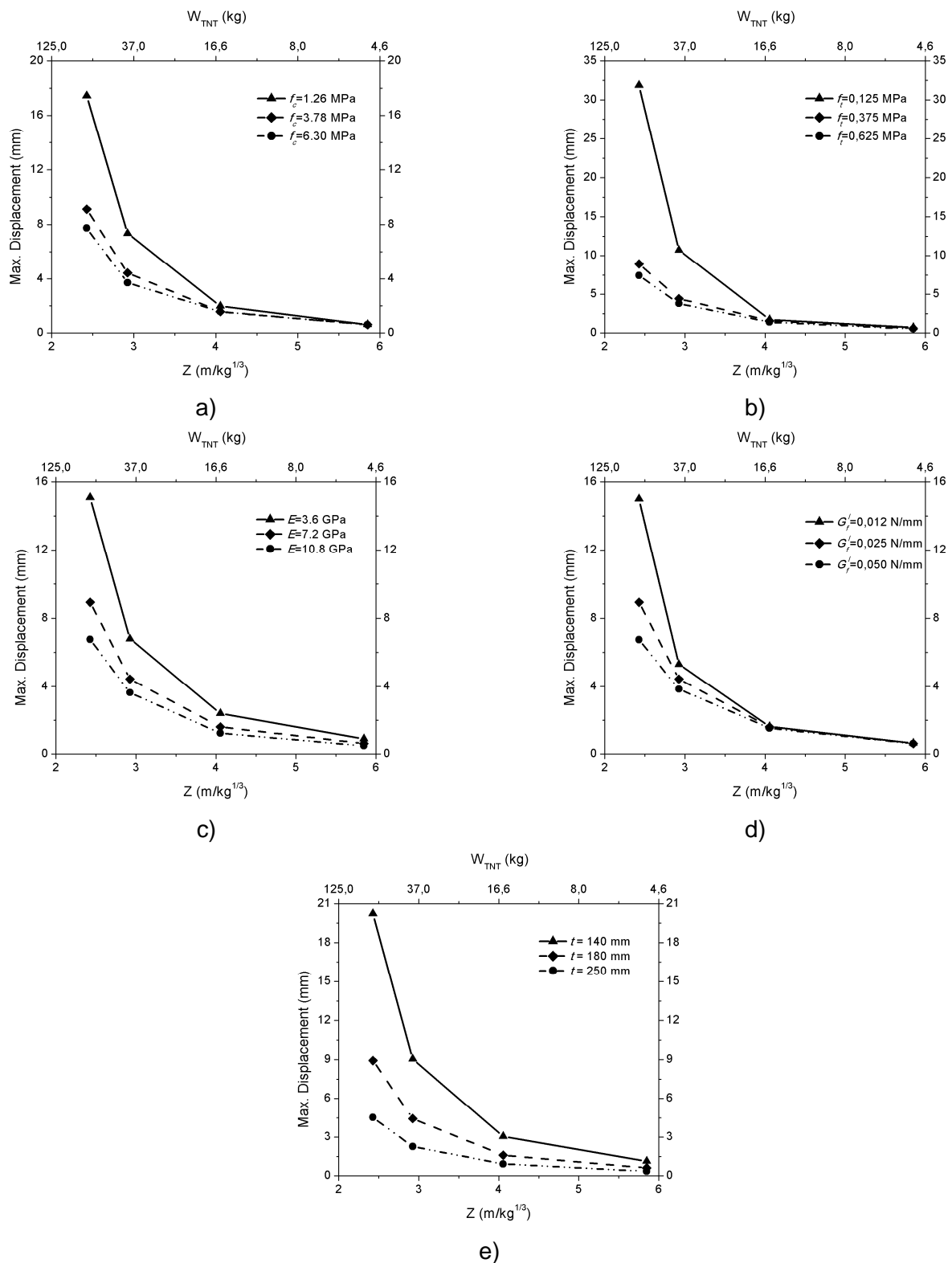

a)

b)

c)

d)

e)

Figure 13. Parametric study on the properties of infill walls subjected to blast loading: a) Compressive strength; b) Tensile strength; c) Young's modulus; d) Mode I-fracture energy; e) Thickness of the wall.

5 CONCLUSIONS

A newly developed test setup for dynamic out-of-plane testing on walls was presented, including the developed sensors and acquisition apparatus. One unreinforced masonry infill panel was tested under blast loading using underwater blast wave generators and the results were presented. The obtained results were used to calibrate a numerical model using ABAQUS Explicit dynamics software. A good agreement between the numerical model and the experimental data was obtained, allowing a more comprised study on this kind of masonry panels under dynamic out-of-plane loading in the form of a parametric study for different loading conditions. There is a point where the increase of the compressive and tensile strength is no longer effective, and the Young's modulus and the wall thickness are the parameters with the higher influence on the behaviour of the wall panel.

These results can be used to created empirical tools, e.g. Pressure-Impulse diagrams, which can provide the designers with simple tools where, according to different loading conditions, the response of the wall panel can be estimated. This information can be crossed with available standards where damage limits are specified for these elements [25]. In order to have larger available experimental data, additional wall are being prepared for testing with different explosive weights and different reinforcement solutions.

REFERENCES
[1] Calvi, G.M., Bolognini, D.: *Seismic response of reinforced concrete frames infilled with weakly reinforced masonry panels.* Journal of Earthquake Engineering, 5 (2001) 2, 153-185.

[2] Wu, C., Hao, H.: *Safe scaled distance for masonry infilled RC frame structures subjected to airblast loads.* Journal of Performance of Constructed Facilities, 21 (2007) 6, 422-431.

[3] Gilbert, M., Hobbs, B., Molyneaux, T.C.K.: *The performance of unreinforced masonry walls subjected to low-velocity impacts: experiments.* International Journal of Impact Engineering, 27 (2002), 231-251.

[4] Mayrhofer, C.: *Reinforced masonry walls under blast loading.* International Journal of Mechanical Sciences, 44 (2002), 1067-1080.

[5] Grote, D., Park, S., Zhou, M.: *Dynamic behaviour of concrete at high strain rates and pressures.* Journal of Impact Engineering. 25 (2001) 9, 869-886.

[6] Ngo, T., Mendis, P., Hongwei, M., Mak, S.: *High strain rate behaviour of concrete cylinders subjected to uniaxial compressive impact loading.* In: Proc. of the 18th Australasian Conference on Mechanics of Structures and Materials. Australia 2004.

[7] Hao, H., Tarasov, B.G.: *Experimental study of dynamic material properties of clay brick and mortar at different strain rates.* Australian Journal of Structural Engineering. 8 (2008), 117-132.

[8] Pereira, J.M., Dias, A., Lourenço, P.B.: *Dynamic properties of clay brick at different strain rates.* In: Proc. of the 12th Canadian Masonry Symposium. Canada 2013.

[9] Tavares, B., Mendes, R., Plaksin, I. Campos, J., Santos, P.M.S., Duarte, B.P.M., Oliveira, N.M.C., Pereira, J.M., Lourenço, P.B.: *Prediction and experimental results of confined underwater blasting generators.* In: Proc. of the 2nd Korean International Symposium on High Energy Materials – KISHEM. Korea 2012.

[10] Ambrósio, J., Ferreira, R., Mendes, R., Campos, J., Pereira, J.M., Lourenço, P.B.: *Prediction and experimental results of confined underwater blasting generators.* In: Proc. of the 44th International Conference of the Fraunhofer ICT, Germany 2013.

[11] Pereira, M.F.P., Pereira, M.F.N., Ferreira, J.E.D., Lourenço, P.B.: *Behaviour of damaged masonry infill panels in RC frames subjected to out of plane loads*. In: Proc. of the 7th International Conference on Analytical Models and New Concepts in Concrete and Masonry Structures. Poland 2011.

[12] Pereira, M.F.P.: Avaliação do desempenho das envolventes dos edificios face à acção dos sismos (in Portuguese). PhD-Thesis, University of Minho, 2013. Department of Civil Engineering: Guimarães 2013.

[13] *ABAQus User Manual*, Dassault Systems Simulia Corporation, Providence USA, 2010.

[14] Cabello, B.: *Dynamic stress analysis of the effect of air blast wave on stainless steel plates*. Msc-Thesis, Faculty of Rensselaer Polytechnic Institute 2011.

[15] Jacinto, A.C., Ambrosini, R.D., Danesi, R.F.: *Experimental and computational analysis of plates under air blast loading*. International Journal of Impact Engineering. 25 (2001) 10, 927-947.

[16] Heidarpour, A., Bradford, M.A., Liu, J.: *Steel arches subjected to blast loading: a non-discretization analysis approach*. Applied Mathematical Modelling. 36 (2012) 9, 3971-3984.

[17] Zheng, Y., Taylor, S., Robinson, D.: *Nonlinear finite element analysis of masonry arch bridges reinforced with FRP*. In: Proc. of the 6th International Conference on Arch Bridges – ARCH'10. China, 2010.

[18] Al-Gohi, B.H., Demir, C., Ilki, A., Baluch, M.H., Rahman, M.K., Al-Gadhib, A.H.: *Seismic vulnerability of multi-leaf heritage masonry walls using elasto-plastic damage model*. In: Proc. of the International Workshop: Role of research infrastructure in seismic rehabilitation. Turkey, 2012.

[19] Lubliner, J., Oliver, S., Onate, E.: *A plastic-damage model for concrete*. International Journal of Solids and Structures. 25 (1989) 3, 299-326.

[20] Lee, J., Fenves, G.L.: *Plastic-damage model for cyclic loading of concrete structures*. Journal of Engineering Mechanics, 124 (1998) 8, 892-900.

[21] Jankowiak, T., Lodygowski, T.: *Identification of parameters of concrete damage plasticity constitutive model*. Foundations of Civil and Environmental Engineering. 6 (2005) 1, 53-69.

[22] Kmiecik, P., Kaminski, M.: *Modelling of reinforced concrete structures and composite structures with concrete strength degradation taken into consideration*. Archives of Civil and Mechanical Engineering, 11 (2011) 3, 623-636.

[23] Bangash, M.Y.H., Bangash, T.: *Explosions – Resistant buildings: Design analysis and case studies*. Sprinter, Germany 2006.

[24] Cormie, D., Mays, G.C., Smith, P.D.: *Blast effects on buildings*. 2nd edition, Thomas Telford Publications: England 2009.

[25] UFC 3-340-02: *Structures to resist the effect of accidental explosions*. Department of Defence, USA 2008.